Electron Spin Resonance and Chemiluminescence Analyses to Elucidate the Vasodilating Mechanism of Sodium Nitroprusside

Giancarlo Aldini, Federica Pirrone, Mariangela Albertini, Marica Orioli, Angela Piccoli, Silvia Mazzola, Maria Giovanna Clement, and Marina Carini

Istituto di Chimica Farmaceutica e Tossicologica "Pietro Pratesi", Faculty of Pharmacy, University of Milan, Milan, Italy (G.A., M.O., A.P., M.C.); and Dipartimento di Patologia Animale Igiene e Sanità Pubblica Veterinaria, University of Milan, Milan, Italy (F.P., M.A., S.M., M.G.C.)

ABSTRACT

The aim of this study was to elucidate the vasodilating mechanism of sodium nitroprusside (SNP). To do this, SNP was intravenously infused in pigs (1.67 μmol/kg), and the following paramagnetic metabolites were identified by electron spin resonance: 1) nitrosylhemoglobin [HbFe(II)NO] as an index of the bioconservative pathway; 2) transferrin; 3) $[Fe^{(II)}(CN)_5NO]^{3-}$ and $[Fe^{(II)}(CN)_4NO]^{2-}$, the reduced penta- and tetracoordinated intermediates of SNP, respectively; and 4) methemoglobin (met-Hb). The results indicate the following: 1) $\approx$17% of the dose is converted to HbFe(II)NO at the end of infusion; 2) NO administered as SNP does not undergo bioinactivation (oxidative metabolism), because no significant increase of met-Hb was observed; 3) the equilibrium involving the paramagnetic species of SNP is shifted toward HbFe(II)NO, because a significant increase of transferrin but no detection of the reduced paramagnetic intermediates of SNP was observed. The results obtained indicate that the hemodynamic effect induced by SNP is not mediated by HbFe(II)NO, at least under physiological conditions; hence, a direct release of NO from SNP in the vascular target should be considered. To demonstrate this mechanism, endothelial cells were incubated with SNP, and the release of NO was determined by a novel chemiluminescence method. The results indicate that the endothelium is able to metabolize SNP, with the formation of stoichiometric amounts of NO. In conclusion, SNP is rapidly metabolized to HbFe(II)NO, but the pharmacological response is mediated by a direct mechanism of NO release of the parent compound at the cellular target.

Sodium nitroprusside or sodium pentacyanonitrosylferrate $Na_2[Fe^{(III)}(CN)_5NO]$ (SNP) is a potent, rapid-acting vasodilator that is widely used clinically in hypertensive emergencies, heart failure, and for controlled hypotension during surgery. Like other nitrovasodilators, SNP is believed to induce vasodilation at the vascular smooth muscle cell through a putative common intermediate, nitric oxide (NO), which by activating guanylate cyclase, catalyzes cGMP accumulation and the pathways resulting in smooth muscle relaxation and the inhibition of platelet aggregation and adhesion (Murad, 1986; Ignarro, 1989).

SNP spontaneously releases NO both thermally and photochemically (Bates et al., 1991), but it is stable in the dark and in aqueous in vitro physiological media (Rao et al., 1991). Hence, energy absorption induces electron transfer from the Fe^{2+} center to the NO^+ ligand, resulting in the weakening of the Fe-NO bond and subsequent release of NO (Bates et al., 1991). SNP also decomposes to NO in an aqueous environment in the presence of biological reductants, such as thiols, which have been shown to improve the hypotensive potency of SNP (Rao et al., 1991), and ascorbic acid, whose mechanism of NO release has been elucidated (Smith and Dasgupta, 2001). Although the in vivo mechanism of NO release is hypothesized to involve the formation of *S*-nitrosothiols (by reaction with glutathione or cysteine) (Ignarro et al., 1981), the molecular mechanism of NO release is far from being fully elucidated. According to several in vitro studies, carried out in homogenous phase or in cell systems, the SNP bioactivation process would involve the following key steps (Williams, 2003): 1) reduction of Fe^{3+} to Fe^{2+} by reducing agents (ascorbic acid and deoxyhemoglobin); 2) formation of a re-

ABBREVIATIONS: SNP, sodium nitroprusside; Hb, hemoglobin; HbFe(II)NO, nitrosylhemoglobin; ESR, electron spin resonance; Met-Hb, methemoglobin; Oxy-Hb, oxyhemoglobin; SVR, systemic vascular resistances; PVR, pulmonary vascular resistances; CO, cardiac output; MAP, mean arterial pressure; MPAP, mean pulmonary arterial pressure; Fe-NOSR, nonheme iron-nitrosyl-sulfur complex; PBS, phosphate-buffered saline; AUC, area under the curve.

duced pentacoordinated intermediate $[Fe^{(II)}(CN)_5NO]^{3-}$, in equilibrium (by loss of CN^-), with the unstable tetracoordinated form $[Fe^{(II)}(CN)_4NO]^{2-}$; 3) decomposition of $[Fe^{(II)}(CN)_4NO]^{2-}$ and release of NO; and 4) reaction of NO with Hb to give nitrosylhemoglobin [HbFe(II)NO].

This mechanism has been confirmed in erythrocyte lysates, in which formation of the paramagnetic species HbFe(II)NO, generated by transfer of NO to Hb via the tetracoordinated intermediate, has been selectively detected by electron spin resonance (ESR) spectroscopy (Wilcox et al., 1990). The reductive mechanism in SNP bioactivation has been further confirmed in different cell system models. In particular, Rochelle et al. (1994), by incubating SNP with porcine endothelial cells and by using ESR spectroscopy to identify the paramagnetic metabolic species of the drug, demonstrated the formation of the pentacoordinated intermediate and of nitrosylated thiol species (nonheme iron-nitrosyl-sulfur complex, Fe-NOSR), generated by reaction of the tetracoordinated intermediate with membrane thiols. Using a sensitive and specific redox chemiluminescence assay for NO, Kowaluk et al. (1992) reported that SNP is readily metabolized to NO in subcellular fractions of bovine coronary arterial smooth muscle and that the dominant site of metabolism is in the membrane fraction. This led to the isolation of a small membrane-bound protein or enzyme that requires electrogenic cofactors (NADPH, NADH) and cysteine to convert SNP to NO. Hence, although in vitro studies indicate that activation of SNP in mammalian tissues can occur in both erythrocytes with formation of HbFe(II)NO and cell systems with formation of nitrosylated species, no definitive in vivo experimental evidences support this mechanistic hypothesis. At the light of the emerging role of HbFe(II)NO in the transport and delivery of NO (Stamler et al., 1997; Gow et al., 1999; Gross and Lane, 1999; Stamler, 2003), the first aim of this work was to make clear, in an in vivo model based on SNP infusion in pigs, the hematic bioactivation process of SNP and the following drug action mechanisms: 1) the reductive metabolism of SNP, leading to the formation of the penta- and tetracoordinated species; and 2) the vasodilating role of HbFe(II)NO, formed from the tetracoordinated form by nitrosylation of hemoglobin. In addition, to gain a deeper insight into the molecular mechanism of SNP at a cellular level, we also examined the potential of endothelial cells to metabolize SNP to NO using a sensitive and selective chemiluminometric method.

Materials and Methods

Materials. Argon (6.0) and NO were kindly provided by Sapio Industrie Srl (Caponago, Milan, Italy). Hemoglobin from bovine blood, sodium nitroprusside, $K_3Fe(CN)_6$, $CuSO_4$, EDTA, Dulbecco's phosphate-buffered saline (PBS), and Dulbecco's modified Eagle's medium were purchased from Sigma (Sigma-Aldrich S.r.l., Milan, Italy); penicillin and streptomycin, histone acetyltransferase media supplement, and L-glutamine were from Invitrogen (San Giuliano Milanese, Italy). Fetal calf serum was from Celbio (Milan, Italy). Spermine NONOate and calcein acetoxymethyl ester were from Invitrogen (Space Import-Export, Milan, Italy).

Surgery. Eight large white pigs of either gender, weighing 23.50 ± 2.66 kg (S.D.) and approximately 3 months old, were used (Istituto Zooprofilattico Sperimentale della Lombardia e dell'Emilia Romagna, Brescia, Italy). When housed in the animal facility, they were fed a standard diet with free access to water and were deprived of food for 24 h before the experiment. All experiments were conducted in accordance with the Institutional Guidelines for the Care and Use of Laboratory Animals (Dipartimento di Patologia Animale, Igiene e Sanità Pubblica Veterinaria, Sezione di Biochimica e Fisiologia, Università degli Studi di Milano).

The animals were sedated with Domitor (medetomidine; Pfizer, Milan, Italy) at 0.03 mg/kg i.m. and Zoletil 100 (tiletamine-zolazepam; Virbac Srl, Milan, Italy) at 4 mg/kg i.m., and anesthetized with 15 mg/kg of thiopental sodium (Farmitalia, Carlo Erba, Italy) injected into the auricular vein. A steady depth of anesthesia was maintained during the experimental protocol by continuous infusion of a dilute solution of thiopental sodium (9 mg/kg/h). The animals were tied in the supine position on a heated operating table, tracheostomized, and intubated with an endotracheal tube inserted into the lower portion of the extrathoracic trachea. They were then paralyzed with pancuronium bromide (0.2 mg/kg i.v.; Organon Teknika B.V., Boxtel, Netherlands) and mechanically ventilated with room air using a 900C Servo ventilator (Siemens-Elema, Solna, Sweden). Supplementary paralyzing agent was administered when necessary. The baseline ventilator settings consisted of a fixed tidal volume of 0.210 ± 0.05 L and a constant inspiratory flow of 0.350 ± 0.04 L/s. The ratio of inspiratory to total breathing cycle duration was 0.33 ± 0.01. The humidifier was omitted from the inspiratory line; the equipment dead space was 29.5 ml (Albertini and Clement, 1995).

Polyethylene catheters were inserted into the right femoral artery to monitor systemic arterial pressure and into the right femoral vein for drug administration. A balloon-tipped catheter (Pediatric Swan-Ganz 5F) was introduced into the right jugular vein and allowed to float through the right heart to the pulmonary artery, so that pulmonary arterial pressure and pulmonary capillary wedge pressure could be measured. The left jugular vein was surgically isolated for infusion of SNP. Systemic and pulmonary arterial pressures were recorded by connecting the catheters to a fluid-filled capacitance manometer (4–422; Bell & Howell, Windsor, Berks, UK). Cardiac output (CO) was measured by a thermodilution technique (Cardiac Output Computer 701; I.L., Milan, Italy). All signals were calibrated independently and recorded simultaneously on a six-channel pen recorder (polygraph; Nec San-ei Instruments, Tokyo, Japan). Arterial blood samples were analyzed with a blood gas analyzer (system 1302; Instrumentation Laboratory, Milan, Italy). The following parameters were evaluated: partial pressure of oxygen, partial pressure of carbon dioxide, pH, and percentage oxyhemoglobin; systemic (SVR) and pulmonary (PVR) vascular resistances were calculated as MAP/CO and (MPAP-Pw)/CO, respectively, where Pw represents pulmonary capillary wedge pressure, and were expressed as millimeters of mercury per liter per minute.

Experimental Protocol. Pigs were divided into two groups: group 1 ($n = 4$) received only saline solution; group 2 ($n = 4$) received SNP (2.00 mM) in physiological solution, prepared immediately before use and protected from the light exposure for the entire experiment. The solutions were infused through the jugular vein at a flow rate of 0.83 ml/min for 24 min, equivalent to 1.67 μmol/kg by a syringe pump (KD Scientific, Holliston, MA). For HbFe(II)NO and Met-Hb analyses, 5-ml blood samples were drawn from the right femoral vein according to the experimental protocol reported in Fig. 1: after anesthesia (T_{00}); after surgery and immediately before SNP infusion (T_0); after infusion of 816 nmol/kg (half-infusion, T_{HI}), immediately at the end of infusion (T_{EI}), and after SNP infusion: 5 (T_5), 15 (T_{15}), 30 (T_{30}), 60 (T_{60}), 90 (T_{90}), 120 (T_{120}), and 180 min (T_{180}). At each time, 2-ml samples were taken from the right femoral artery for blood gas analysis. The hemodynamic parameters (MAP, MPAP, and heart rate) were recorded continuously, whereas CO, SVR, and PVR were measured at T_0, T_{EI}, T_{15}, T_{30}, T_{60}, T_{90}, T_{120}, T_{150}, and T_{180}.

ESR Analyses of HbFe(II)NO, Met-Hb, and Transferrin. HbFe(II)NO ESR spectra were recorded at 100 K with a Bruker EMX spectrometer (X band) equipped with a high-sensitivity cylindrical cavity (ER4119HS; Bruker, Milan, Italy) as reported previously (Aldini et al., 2004). Concentration of HbFe(II)NO was determined by

double integration of the signal using CuSO$_4$-EDTA as reference standard (Carini et al., 2001; Aldini et al., 2004).

Met-Hb and transferrin were measured by ESR spectroscopy using the following instrumental conditions: microwave frequency, 9.316 GHz; microwave power, 20 mW; modulation frequency, 100 kHz; modulation amplitude, 5 G; number of scans, 10; resolution, 1024 points; sweep time, 21 s; center field, 1400 G. Stock solutions of Met-Hb were prepared by oxidizing Oxy-Hb with a slight molar excess of K$_3$Fe(CN)$_6$ followed by dialysis against 50 mM sodium phosphate buffer, pH 7.4. The concentration of Met-Hb solutions (always expressed per unit of heme) was determined by absorption spectroscopy (Lambda 16; PerkinElmer Life and Analytical Sciences, Monza, Italy) at 700, 630, 576, and 560 nm using the Winterbourn relationship (Winterbourn, 1990). Working standard solutions were prepared by diluting the stock solution with 50 mM sodium phosphate buffer in the range 0.5 to 50 μM. The equation of the calibration curve (range, 0.5–10 μM) was y = 0.4772 $\pm$ 0.012x + 0.1859 $\pm$ 0.074 (r^2 = 0.9973; S.E. of estimate Sy; x = 0.101) and the calculated limits of detection and quantification by ESR were 0.4 and 1.0 μM, respectively. Transferrin ESR signal was double-integrated and expressed as arbitrary units.

Preparation and ESR Analysis of the Paramagnetic Metabolites of SNP. Penta- and tetracoordinated complexes were prepared by using NaBH$_4$ as reducing agent as described previously (Kruszyna et al., 1993). ESR analyses were carried out in the following conditions: microwave frequency, 9.316 GHz; microwave potency 20 mW; modulation frequency 100 kHz; modulation amplitude, 5 G; number of scans, 20; resolution, 1024 points; center field, 3500 G; sweep width, 5000 G. The same operating conditions were used to identify the paramagnetic metabolites of SNP in blood (0.3-ml aliquots).

Data Analysis. All values in the figures and text for HbFe(II)NO and Met-Hb are expressed as means $\pm$ S.D., and those for hemodynamics are expressed as means $\pm$ S.E. The statistical significance of differences between vehicle and SNP-treated animals was done by t test analysis. Statistical analysis was done using Prism for Windows (ver. 3.0; GraphPad Software Inc., San Diego, CA). Significance was taken where $P < 0.05$ (∗), $P < 0.01$ (∗∗), and $P < 0.001$ (∗∗∗).

Cell Cultures and SNP Incubation. EA.hy926 cells were cultured as described previously (Aldini et al., 2003), and cell viability was determined by the calcein acetoxymethyl ester assay (Oral et al., 1998). For incubation experiments with SNP, confluent endothelial cells in 25-cm^2 flasks ($\sim$5.2 $\times$ 10^5 cells/ml) were washed twice with PBS and then incubated in PBS spiked with SNP (0.1, 0.2, and 0.3 mM in PBS, corresponding to 1, 2, and 3 nmol added). During the experiments, the flasks were maintained at 37°C under orbital shaking and protected from light exposure (by covering with aluminum foil).

Chemiluminescent Detection of NO: Flask-Chemiluminometer Connection. NO released from SNP was determined by an ozone-based chemiluminescent assay, using a Sievers Instruments model 280 Nitric Oxide Analyzer (Sievers, Boulder, CO; Sensor Medics, Milan, Italy). Because the apparatus is dedicated to liquids sampling (plasma or tissue homogenates for determination of ni-

trites/nitrates), it was suitably adapted in our laboratory for the NO detection directly from the incubated cells. Figure 2 reports a schematic representation of the apparatus used. The flasks were maintained under a constant flux of helium purged through distilled water and connected to the flask through a Teflon tube sealed with the flask screw caps. The flask outlet was connected to the reaction chamber of the chemiluminometer through a second Teflon tube. Cells were maintained at 37°C through heater coil water connected to a thermostated circulating water bath.

NO Quantitation: Calibration Curve. Spermine NONOate was used as a calibrating standard, because its thermal decomposition is known to release NO at a constant rate (Maragos et al., 1991). Stock solutions of spermine NONOate (0.6 mM), prepared in 0.01 M NaOH, were diluted with 0.01 M NaOH to obtain working solutions at the final concentrations of 0.05, 0.075, 0.1, 0.2, and 0.3 mM. Aliquots (10 μl) of each working solution were injected into the reaction vessel containing PBS (6 ml) maintained at 37°C. The concentration range for calibration, expressed as nanomoles of injected spermine NONOate, was 0.5 to 3 nmol, corresponding to 0.95 to 5.7 nmol NO. Calibration standards were analyzed in duplicate in three independent runs. The calibration curves were constructed by weighted (1/x2) least-square linear regression analysis of the peak area against analyte concentration (nanomoles of NO). The lower limit of quantitation was determined as the lowest concentration with values for precision and accuracy within $\pm$20% and a signal-to-noise ratio of the peak areas $\geq$10. The extraction efficiency of NO from the flask was determined by comparing the chemiluminometric response of spermine NONOate added to the flask to that of an equimolar concentration added to the conventional reaction vessel (extraction efficiency, 100%). The overall absolute extraction efficiency was measured as the ratio of the two areas under the curve (AUCs) obtained, and expressed as percentage.

Results

Identification of Blood Paramagnetic Species. Figure 3 shows a representative ESR spectrum (A) of a blood sample after anesthesia and before surgery (T$_{00}$), with three main signals attributed to Met-Hb (g = 5.714), transferrin (g = 4.110) (top), and to the Cu^{2+} of ceruloplasmin (g = 2.054). As observed in previous studies (Aldini et al., 2004), no signal was detected for HbFe(II)NO (see the display of the 3100- to 3500-G region on the right) to confirm that the endogenous levels in pigs are lower than the limit of ESR detection (0.25 μM). In all of the animals subjected to 30-min equilibrium after surgery and before vehicle or SNP infusion (time T$_0$), the signal relative to HbFe(II)NO becomes detectable (Fig. 3, spectrum B), as evidenced by the presence of the three lines of the HbFe(II)NO signal centered at g = 2.009 (indicated by the arrows in the 3100- to 3500-G region spectrum). In Fig. 3 are also reported the ESR spectra of blood samples taken 12 (T$_{HI}$) and 24 min (T$_{EI}$) after the start of SNP infusion (spectra
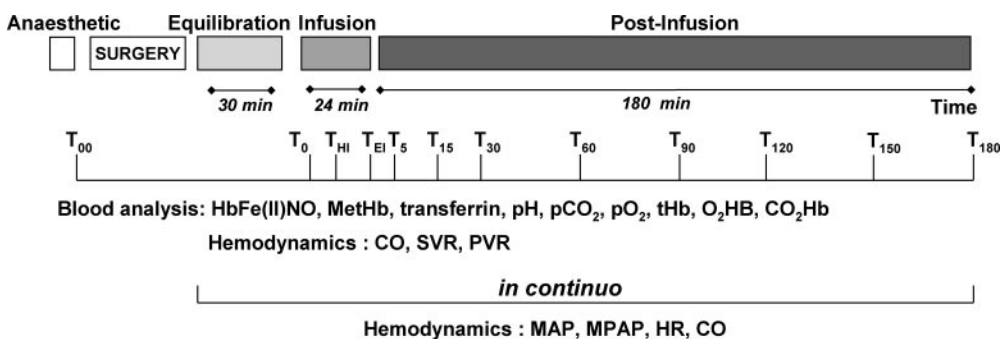
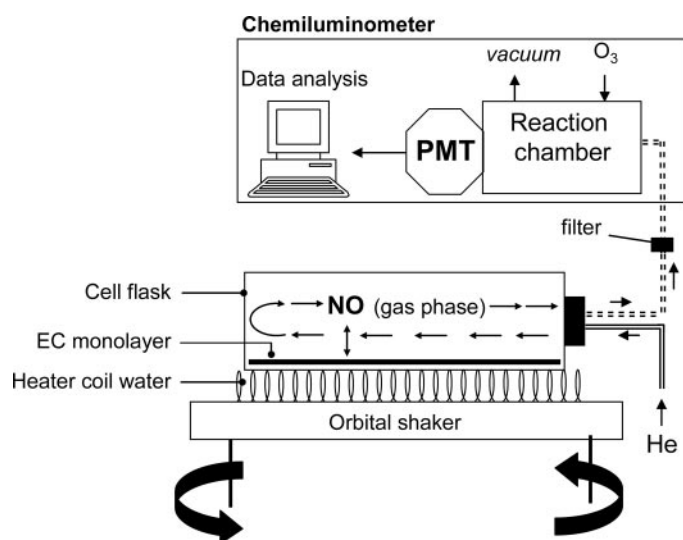**Fig. 1.** SNP infusion in pigs: experimental protocol.

Fig. 2. Schematic representation of the modified chemiluminometric apparatus for determination of NO released from endothelial cells incubated with SNP. Cells were maintained at 37°C through heater coil water, and the NO generated by endothelial cells in equilibrium with the gas phase is stripped by a constant flux of helium. The flask outlet is connected to the reaction chamber of the chemiluminometer through a Teflon tube. EC, endothelial cells (EA.hy926); PMT, photomultiplier tube.

C and D), in which the additional signal at $g \approx 2.00$ significantly increases with respect to the T_0. Attribution was achieved by subtracting the T_{00} spectrum from those recorded at T_0, T_{HI}, and T_{EI}. The difference spectra (Fig. 4A reports that relative to T_{00} subtracted from T_{EI}) shows two distinct signals that are significantly increased with respect to T_0: at $g = 4.110$, attributed to the Fe^{3+} of transferrin (whose increase indicates iron release from SNP), and a signal centered at $g = 2.009$ with a hyperfine coupling constant $A_N = A_X = 17$ G, which overlaps that reported for the T-state of nitrosylated purified α-subunits of hemoglobin (Fig. 4, B and C) (Yonetani et al., 1998). The increase of the HbFe(II)NO signal after SNP infusion was evident in all the treated animals, whereas no significant differences in the HbFe(II)NO signal intensity was observed either during or after the vehicle infusion.

Because early in the in vitro reaction of SNP with erythrocyte lysates the ESR signals of both $[Fe^{(II)}(CN)_5NO]^{3-}$ and $[Fe^{(II)}(CN)_4NO]^{2-}$ species were observed (Wilcox et al., 1990), we prepared and analyzed by ESR the relative standards to verify whether their formation takes place also in vivo. ESR analyses indicate that no detectable signals relative to the penta- or tetracoordinated species were detected in blood samples withdrawn during or after SNP infusion.
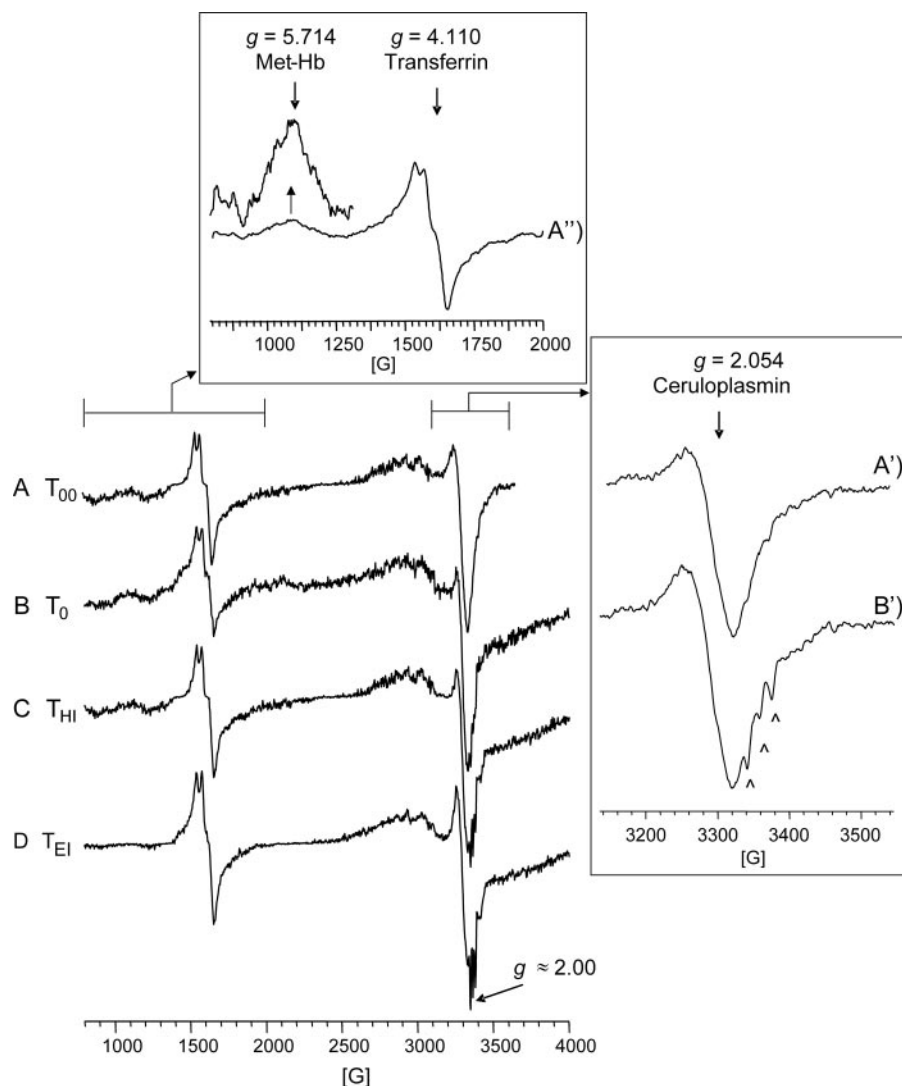

Fig. 3. Representative ESR spectra of blood samples drawn before (T_{00}, A; T_0, B) and during (T_{HI}, C; T_{EI}, D) SNP infusion. Spectra A through D were recorded by using a wide scan range (center field of 2400 G, sweep width of 3200 G) to identify all the paramagnetic blood metabolites and the following instrumental conditions: microwave power, 20 mW; modulation frequency, 100 kHz; modulation amplitude, 5 G; number of scans, 1; resolution, 1024 points. Met-Hb and transferrin (top box, A″) were determined by setting the center field at 1400 G (sweep width of 1200 G) and increasing the number of scans to 20. For a better visualization, the signal relative to Met-Hb has been magnified in respect to transferrin. Spectra in the right box were recorded using a center field of 3300 and are relative to T_{00} (A′) and T_0 (B′). The arrows in spectrum B′ indicate the appearance of three lines centered at $g = 2.009$ and attributed to HbFe(II)NO.

Nitrosylhemoglobin Levels. Figure 5 shows the time course of HbFe(II)NO formation from vehicle and SNP-treated animals. Quantitative analysis indicates a significant increase in the blood levels of all of the pigs after surgery (T_0), which increased to 1.30 ± 0.91 μM ($n = 8$), probably because of endothelial activation induced by arterial and venous catheterization. HbFe(II)NO levels did not significantly change during and after vehicle infusion and remained in a concentration range between 0.87 and 1.45 μM. After 12 min of SNP infusion, HbFe(II)NO content increased from 1.18 ± 0.26 to 3.07 ± 0.15 μM ($P < 0.05$), reaching a C_{max} of 4.48 ± 1.21 μM at the end of infusion (T_{EI}) (0.80 ± 0.52 μM in vehicle-treated animals; $P < 0.01$). The kinetics of HbFe(II)NO at the subsequent observation times confirm an exponential decay and a half-life ($t_{1/2}$) of 14 min, as demonstrated previously in pigs after infusion of a saturated NO solution (Aldini et al., 2004). The HbFe(II)NO blood content reached approximately the preinfusion value 30 min after the stop of the infusion (1.48 ± 0.61 μM; $P > 0.05$) and remained almost stable up to the last observation time (T_{180}).

Methemoglobina and Transferrin Levels. In previous studies, we demonstrated that plasma NOx (nitrite + nitrate) can not be used in pigs as a reliable marker of the oxidative metabolism of NO, because the very high basal levels (≈ 100 μM at T_0, 2- to 3-fold greater than those found in other animal species and in humans) do not allow accurate measurement of minimal variations because of exogenous NO (Aldini et al., 2004). For this reason, Met-Hb, a product of the oxidative reaction between Oxy-Hb and NO (Gladwin et al., 2000), can be considered a valid and alternative marker on NO oxidative metabolism in pigs.

The results reported in Fig. 5 indicate that basal levels (T_0) of Met-Hb are 6.71 ± 0.33 μM, a value that remained almost stable in vehicle-treated animals during and after saline infusion. Unlike levels observed after NO administration (Aldini et al., 2004), SNP infusion did not affect Met-Hb levels; no significant differences were observed in the drug-treated group at all observation times.

Figure 5 shows the time course of the ESR signal relative to blood transferrin in vehicle- and SNP-treated animals.

Saline infusion did not modify transferrin levels, and the ESR signal at all postinfusion times were comparable with those at T_0. In SNP-treated animals, a time-dependent increase of the transferrin signal was recorded, which was already significant at half-infusion (T_{HI}) and plateaued at T_{EI}. The levels significantly decreased only at T_{120} and then gradually returned to preinfusion levels.

Hemodynamic Effects. As shown in Fig. 6, SNP infusion evoked an immediate and significant ($P < 0.05$) decrease in mean systemic and pulmonary blood pressures. The acute hypotensive state occurring with SNP infusion was compensated by adequate hemodynamic responses: the decreased blood pressure was matched by a significant increase in heart rate and a moderate elevation in cardiac output. Although the latter parameter could not be measured at T_{HI} while the hypotensive peak occurred, so as not to interfere with the drug infusion, the relative values achieved at T_{EI} showed a trend of increase consistent with the physiological events that intravenous sodium nitroprusside is reported to rouse. In other words, SNP acted directly on vascular smooth muscle, causing vasodilation. As was expected, during the hypotensive period, systemic and pulmonary vascular resistances also decreased in SNP group, although to levels which were not statistically significant; in particular, there was a reduction in SVR of 31% and of 15% in PVR.

In Vitro Studies: Method Development and Validation. The first step of the in vitro studies was to develop and validate a suitable methodology to monitor NO release from endothelial cells incubated with SNP. To do this, the flask containing the cell monolayer was maintained under a constant flux of helium to guarantee the extraction and transport of NO to the chemiluminometric system. Extraction efficiency from the flask was calculated using spermine NONOate in PBS as a standard because this polyamine/NO adduct spontaneously decomposes to NO at 37°C and pH 7.4, with a known rate constant for decomposition (half-life at 37°C = 39 min) and with a stoichiometric conversion factor of 1.9 (Maragos et al., 1991). Figure 7 shows the chemiluminometric signal (recorded in continuo) obtained by adding 1.5 nmol spermine NONOate to 6 ml of PBS in the 25-cm^2 flask.
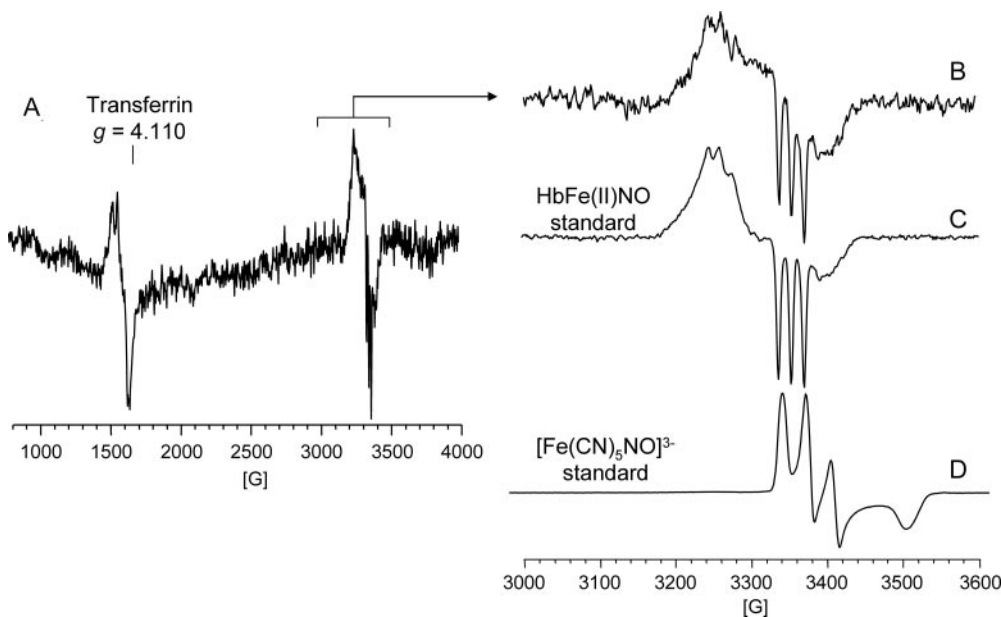

Fig. 4. Representative difference spectra relative to T_{00} subtracted from T_{EI} and recorded with a scan range 800 to 4000 G (A) and 3000 to 3600 G (B). Spectra C and D are relative to standard samples of HbFe(II)NO and $[Fe^{(II)}(CN)_5NO]^{3-}$, respectively.

A rapid increase of the NO signal is obtained immediately after injection, whose intensity, fairly constant for approximately 20 min, progressively and linearly decreases with time, to reach basal levels after 220 min.

The instrumental responses obtained by injecting the spermine NONOate working solutions were integrated and calculated as AUCs. The calibration curves were fit over the entire calibration ranges (1.41–5.70 nmol injected), using a $1/x^2$ weighted quadratic fit and showed good linearity with correlation coefficient (r^2) greater than 0.998. The equation for the calibration lines was $y = 160,700 \pm 21,240x - 107,000 \pm 68,010$. The AUC values relative to each concentration level were comparable with those obtained by directly injecting the spermine NONOate working solutions into the conventional reaction vessel for liquids sampling (relative S.D. ≤10%), to indicate an almost superimposable extraction efficiency (≈100%).

SNP Incubation with Endothelial Cells. Figure 8A reports the time course of the chemiluminometric response obtained by incubating endothelial cells at 37°C in the absence of any added substrate (cell viability was unaffected up to 180 min of incubation). As expected, no release of NO was detected at up to 180 min of incubation as a result of the anaerobic conditions generated by a constant flux of helium that does not permit the endogenous generation of NO by NO synthase. A similar chemiluminescent profile was seen by
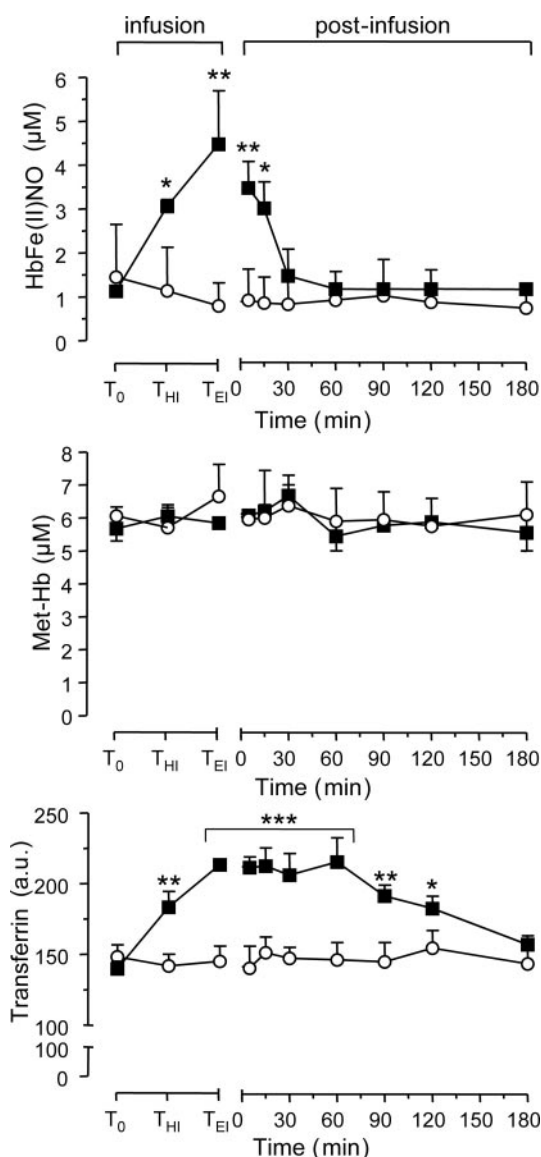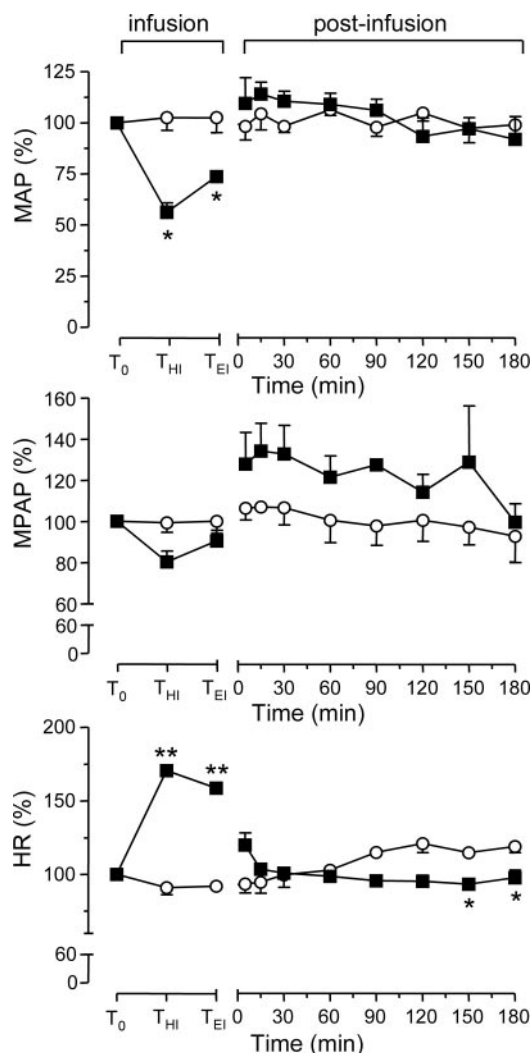
Fig. 5. Blood levels of HbFe(II)NO, Met-Hb and time course of transferrin ESR signal in pigs treated with saline (○) or SNP solution (■). The data are represented as the mean ± S.D. ($n = 4$). t Test analysis was used to compare the two groups at each time point (∗, $P < 0.05$; ∗∗, $P < 0.01$; ∗ ∗∗, $P < 0.001$).

Fig. 6. Time-dependent effects of SNP (■) and vehicle (○) infusion on MAP, MPAP, and HR. Values are the mean percentage ± S.E. t Test analysis was used to compare the two groups at each time point (∗, $P < 0.05$; ∗∗, $P < 0.01$).
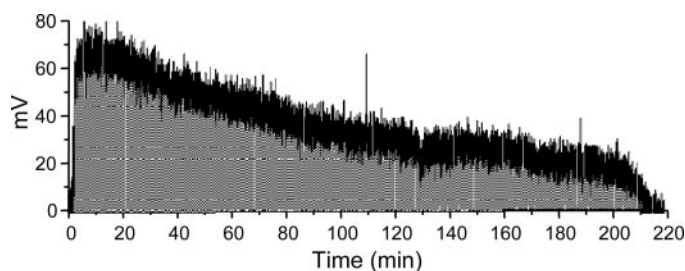
Fig. 7. Calibration of the chemiluminometric system for quantitative analysis of NO: time course of NO release obtained by adding 1.5 nmol of spermine NONOate to 6 ml of PBS in the 25-cm² flask.

incubating SNP (2 nmol) in PBS and in the absence of endo-thelial cells, thus to exclude any artifactual and spontaneous release of NO from SNP (Fig. 8B). When 1 and 2 nmol of SNP were added to the cell monolayer (Fig. 8, C and D, respec-tively), a dose-dependent increase in the NO signal was ob-served already after a few minutes of incubation to indicate the ability of endothelial cells to catalyze NO release from the drug. The time course of NO formation is similar at both dosages: maximal formation is observed after 30 min of in-cubation to slowly decrease and return to basal levels within 130 min (1 nmol) and 180 min (2 nmol). Cell viability was not affected at any of the SNP doses tested.

Because it is known that SNP spontaneously releases NO photochemically (Bates et al., 1991), at the end of the exper-iments ($\approx$180 min), the reaction flasks were illuminated by a tungsten lamp to evaluate the completeness of the SNP bio-transformation process. As shown in Fig. 8 (C and D), no further increase of the NO signal was detected after the light exposure, with respect to an SNP solution (C, inset), to indi-cate the ability of endothelium to induce a total conversion of SNP to NO. Quantitative analysis indicates that SNP bio-conversion to NO is dose-dependent and accounts for more than 75% of the incubated doses. The remaining 25% is very likely to be converted to other metabolic species such as *S*-nitrosothiols or Fe-NOSR complexes (Wilcox et al., 1990).

Discussion

It has been demonstrated previously that under aerobic and anaerobic conditions, SNP can undergo a one-electron exchange reaction with hemoglobin, which produces Met-Hb

Fig. 8. Time course of NO release determined by chemiluminescence analysis in the following experimental conditions: cultured endothelial cells (A); PBS spiked with 2 nmol of SNP (B); cultured endothelial cells incubated with 1 nmol (C) and 2 nmol (D) of SNP.

and cyanide. This one-electron reduction of SNP is required for NO release and its transfer to other heme(II). The reac-tion between SNP and Hb has been demonstrated to occur both in solution and in intact or lysate red blood cells with the formation of nitrosylated Hb, but no evidence for its in vivo occurrence has been provided until now (Wilcox et al., 1990; Kruszyna et al., 1993).

The results reported herein demonstrate for the first time, in an in vivo animal model, that SNP is rapidly bioconverted in blood with the release of iron and HbFe(II)NO formation. ESR analysis of blood samples from SNP-infused pigs pro-vided evidence that transferrin and HbFe(II)NO are the only detectable paramagnetic metabolites generated in vivo. Al-though no quantitative data have been generated in this study, the increase in the transferrin ESR signal during SNP infusion can be considered an unequivocal index of a rapid compartmentalization of released Fe(II) into transferrin, de-riving from the decomposition of $[Fe(II)(CN)_4]^{2-}$. Regarding the paramagnetic metabolites of SNP, neither $[Fe(II)(CN)_4]^{2-}$ and $[Fe(II)(CN)_5]^{3-}$ were detected during or af-ter the SNP infusion, suggesting that the reduced penta- and tetracoordinated SNP species are transient metabolic inter-mediates and that the following equilibria are, in vivo, mainly shifted toward the following reaction products:

1. $[Fe^{(III)}(CN)_5NO]^{2-} + e^- \leftrightarrows [Fe^{(II)}(CN)_5NO]^{3-}$
2. $[Fe^{(II)}(CN)_5NO]^{3-} \leftrightarrows [Fe^{(II)}(CN)_4NO]^{2-} + CN^-$
3. $[Fe^{(II)}(CN)_4NO]^{2-} + HbFe^{(II)} \leftrightarrows [Fe^{(II)}(CN)_4]^{2-} + HbFe^{(II)}NO$

Reaction 2 generates cyanide, the toxicity of which is well documented, and the possible cyanide poisoning at excessive total SNP doses or infusion rates (Friederich and Butter-worth, 1995). Anyway, cyanide is rapidly cleared by enzy-matic transsulfuration reactions (rhodanase and mercapto-pyruvate sulfurtransferase) (Nagahara et al., 1999; Scheffler, 2001) and nonenzymatic means in erythrocytes, mainly by interaction with both ferric and ferrous heme proteins, giving highly stable complexes, values of the association equilib-rium constant being higher than 10^5 M^{-1} (Milani et al., 2004). Hence, by considering the ability of most adults to detoxify by the enzymatic routes up to 50 mg of total SNP (Friederich and Butterworth, 1995) and the high reactivity toward heme proteins (not determined because it was outside the aim of this work), we can reasonably assume that the in vivo rapid subtraction of cyanide would shift equilibrium (reaction 2) in favor of the tetracoordinated form, which is obligatory for NO transfer. The $[Fe^{(II)}(CN)_4NO]^{2-}$ species is in turn in equilibrium with HbFe(II)NO and with $[Fe^{(II)}(CN)_4]^{2-}$ species. By considering the HbFe(II) excess, the favorable kinetics of HbFe(II)NO formation ($k_{on} = 10^7$ M^{-1} s^{-1}) (Yonetani et al., 1998), and the metabolic conver-sion of $[Fe^{(II)}(CN)_4]^{2-}$ with transferrin formation, we can deduce that the equilibrium (reaction 3) is mainly shifted toward the reaction products.

Hemodynamic parameters indicate that SNP induces a significant reduction in systemic and pulmonary arterial pressure, the vasodilating effect started from the beginning of the infusion (T_0). In particular, the infusion of SNP pro-duced a marked lowering in mean arterial blood pressure, which decreased during the infusion and returned to prein-jection values upon cessation of infusion, increase in cardiac
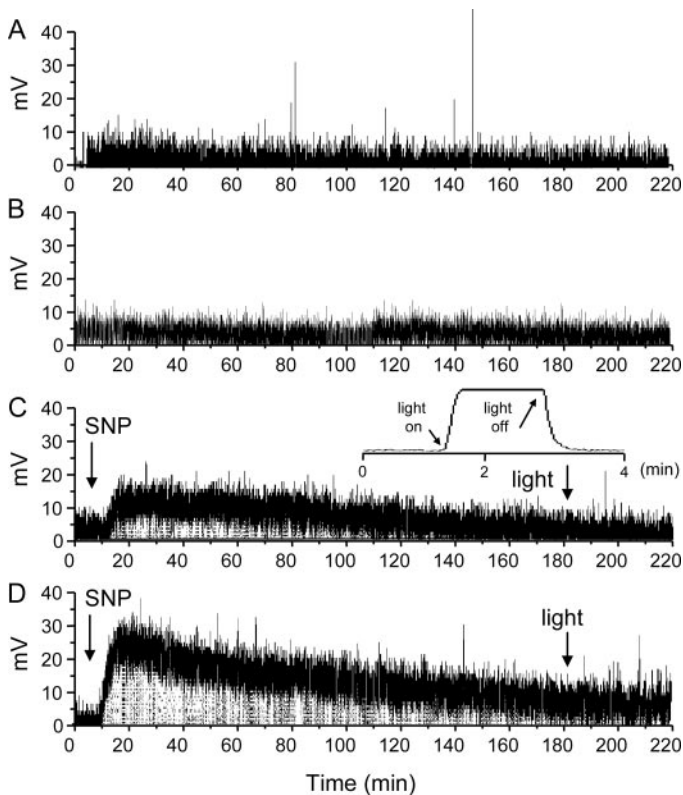
output, and decrease in peripheral resistance. The vasodilating effect induced by SNP could be mediated by HbFe(II)NO, a stable bioactive storage form of NO, able to transport the vasoactive mediator distally from the site of administration (Aldini et al., 2004). By considering a total blood volume in pig of approximately 2 L, and the amount of HbFe(II)NO determined at the end of infusion (C_{max} 4.15 $\pm$ 0.69 versus 0.80 $\pm$ 0.52 μM), the efficiency of SNP bioconversion to HbFe(II)NO accounts for $\approx$17% of the administered dose ($\approx$40 μmol in 24 min). Taking into account that 5 nM (EC_{50}) is the NO concentration required to induce a vasoactive response in aortic ring (Brandes et al., 2000), the amount of HbFe(II)NO after the SNP injection should be high enough to potentially induce a vasoactive response. However, in previous experiments carried out in the same animal model, we found that an equimolar dose of a saturated NO solution (24-min infusion in pigs) was much more efficiently converted to HbFe(II)NO (equivalent to 40% of the administered dose) but did not induce any hemodynamic response under physiological conditions (Aldini et al., 2004). Taken together, these data exclude any role for HbFe(II)NO in the vasodilating mechanism of SNP and further strengthen the hypothesis that NO captured by deoxygenated hemes is not an effective way to subsequently transduce NO bioactivity, at least in physiological conditions, as confirmed by the slow off-rate ($\approx$10^{-3} to 10^{-5}) of HbFe(II)NO (Kim-Shapiro et al., 2006).

Although methemoglobinemia is a well-known side effect of SNP infusion, in our experimental conditions, no significant increase of Met-HB was observed during and after SNP infusion. The data are explained by considering the dose used (1.67 μmol/kg), which is significantly lower in respect to the dose (more than 46 μmol/kg) typically required to generate 10% methemoglobinemia (Friederich and Butterworth, 1995). Met-Hb, besides being the product of the redox reaction between Heme(II) and SNP, is also produced by the oxidative reaction of Oxy-Hb and NO and for this reason is considered to be a marker of NO bioinactivation by oxidative metabolism (Gladwin et al., 2000). We found previously that an equal dose of a genuine NO solution (1.67 μmol/kg) induced a significant increase of Met-Hb in respect to the basal content and that the amount of NO entering the oxidative metabolism was $\approx$25%. Taken together, the data indicate that NO administered as SNP does not undergo a significant oxidative-dependent bioinactivation. The reduced tetracoordinated species probably preferentially donates NO to deoxyhemoglobin with formation of the nitrosyl derivative rather then to the oxygenated form with the formation of Met-Hb.
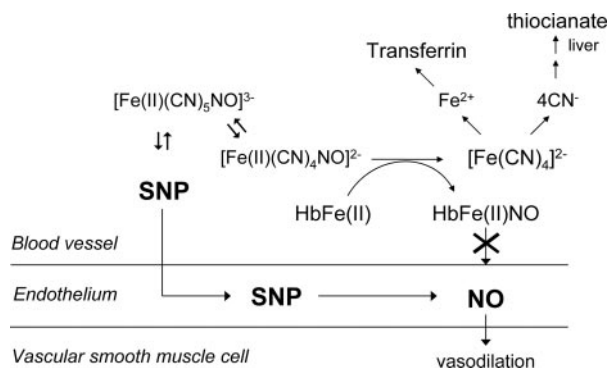
By considering that HbFe(II)NO is not involved in the vasodilating mechanism of SNP, a direct release of NO from SNP in the vascular target should be considered to explain the vasodilating mechanism. This also takes into account, on the basis of HbFe(II)NO and Met-Hb levels, that a significant proportion of infused SNP does not undergo a metabolic conversion in blood, and it is potentially available to reach the vascular district and to be bioactivated at cellular level. This hypothesis is further sustained by considering that SNP undergoes a 30% extraction from the blood during a single passage through peripheral vascular beds in the rat in vivo (Kreye and Reske, 1982). To act as a vasodilating agent, SNP might be metabolized by vascular tissues to NO, as already demonstrated in smooth muscle cells (Kowaluk et al., 1992). These considerations prompted us to investigate in vitro the ability of vascular endothelial cells to release NO from SNP. Through a novel developed (and suitably validated) experimental model, based on the sensitive chemiluminometric detection of released NO, it was possible to demonstrate that more than 70% of the incubated SNP dose is converted by endothelial cells to NO. Because of the claimed fundamental role of the sulfhydryl-containing compounds (glutathione and cysteine) in inducing NO release form SNP, we can reasonably postulate that NO generation at an endothelial level might follow the mechanism recently proposed by Grossi and D'Angelo (2005). An electron-transfer process can be invoked as the key step, which leads to the formation of the reduced SNP radical and the corresponding *S*-nitrosothiol, the ending product of NO that can be considered the real storage and transporter of NO. Under anaerobic conditions, *S*-nitrosothiols can undergo thermal decomposition by homolytic cleavage of the S-N bond that leads to nitric oxide and sulfanyl radicals in a reversible reaction. As a consequence, the decomposition rate is strongly decreased by the presence of endogenous and/or exogenous nitric oxide (Grossi and Montevecchi, 2002). Because in our conditions NO is continuously removed by the stream of helium, the decomposition rate is increased, favoring the escape of NO from the reaction vessel. The remaining 25% of unrecovered NO is very likely to be converted to other metabolic species, such as Fe-NOSR, as demonstrated previously by Rochelle et al. (1994) or is conserved as *S*-nitrosothiols (not determined in this study).

In conclusion, the results of the in vivo studies demonstrate that NO released in the blood compartment and transported as HbFe(II)NO is not involved in the vasodilating mechanism. In vitro studies clearly indicate that endothelium is able to metabolize SNP, with the formation of stoichiometric amounts of NO, the agent responsible for vasodilation. Hence, we can postulate that the amount of the administered drug in our in vivo model that escapes the bioconservative pathway (more than 80% of the dose) reaches the endothelium: this means that the pharmacological response of SNP is mediated by a direct mechanism of NO release/metabolization of the parent compound at the cellular target. Figure 9 summarizes the proposed metabolic scheme for SNP bioactivation and vasodilating mechanism.

Fig. 9. Proposed metabolic scheme for SNP bioactivation and vasodilating mechanism.

References

Albertini M and Clement MG (1995) Inhaled nitric oxide reverses PAF-dependent bronchoconstriction in the pig. *Prostaglandins Leukot Essent Fatty Acids* **52:**373–380.

Aldini G, Carini M, Piccoli A, Rossoni G, and Facino RM (2003) Procyanidins from grape seeds protect endothelial cells from peroxynitrite damage and enhance

endothelium-dependent relaxation in human artery: new evidences for cardio-protection. *Life Sci* **73:**2883–2898.

Aldini G, Orioli M, Maffei Facino R, Giovanna Clement M, Albertini M, Mazzola S, Pirrone F, and Carini M (2004) Nitrosylhemoglobin formation after infusion of NO solutions: ESR studies in pigs. *Biochem Biophys Res Commun* **318:**405–414.

Bates JN, Baker MT, Guerra R Jr, and Harrison DG (1991) Nitric oxide generation from nitroprusside by vascular tissue. Evidence that reduction of the nitroprusside anion and cyanide loss are required. *Biochem Pharmacol* **42:**S157–165.

Brandes RP, Kim D, Schmitz-Winnenthal FH, Amidi M, Godecke A, Mulsch A, and Busse R (2000) Increased nitrovasodilator sensitivity in endothelial nitric oxide synthase knockout mice: role of soluble guanylyl cyclase. *Hypertension* **35:**231–236.

Carini M, Aldini G, Stefani R, Orioli M, and Facino RM (2001) Nitrosylhemoglobin, an unequivocal index of nitric oxide release from nitroaspirin: in vitro and in vivo studies in the rat by ESR spectroscopy. *J Pharm Biomed Anal* **26:**509–518.

Friederich JA, Butterworth JF 4th (1995) Sodium nitroprusside: twenty years and counting. *Anesth Analg* **81:**152–162.

Gladwin MT, Ognibene FP, Pannell LK, Nichols JS, Pease-Fye ME, Shelhamer JH, and Schechter AN (2000) Relative role of heme nitrosylation and β-cysteine 93 nitrosation in the transport and metabolism of nitric oxide by hemoglobin in the human circulation. *Proc Natl Acad Sci USA* **97:**9943–9948.

Gow AJ, Luchsinger BP, Pawloski JR, Singel DJ, and Stamler JS (1999) The oxyhemoglobin reaction of nitric oxide. *Proc Natl Acad Sci USA* **96:**9027–9032.

Gross SS and Lane P (1999) Physiological reactions of nitric oxide and hemoglobin: a radical rethink. *Proc Natl Acad Sci USA* **96:**9967–9969.

Grossi L and D'Angelo S (2005) Sodium nitroprusside: mechanism of NO release mediated by sulfhydryl-containing molecules. *J Med Chem* **48:**2622–2626.

Grossi L and Montevecchi PCA (2002) Kinetic study of S-nitrosothiol decomposition. *Chem Eur J* **8:**380–387.

Ignarro LJ, Lippton H, Edwards JC, Baricos WH, Hyman AL, Kadowitz PJ, and Gruetter CA (1981) Mechanism of vascular smooth muscle relaxation by organic nitrates, nitrites, nitroprusside and nitric oxide: evidence for the involvement of S-nitrosothiols as active intermediates. *J Pharmacol Exp Ther* **218:**739–749.

Ignarro JL (1989) Biological actions and properties of endothelium-derived nitric oxide formed and released from artery and vein. *Circ Res* **65:**1–21.

Kim-Shapiro DB, Schechter AN, and Gladwin MT (2006) Unraveling the reactions of nitric oxide, nitrite, and hemoglobin in physiology and therapeutics. *Arterioscler Thromb Vasc Biol* **26:**697–705.

Kowaluk EA, Seth P, and Fung HL (1992) Metabolic activation of sodium nitroprusside to nitric oxide in vascular smooth muscle. *J Pharmacol Exp Ther* **262:**916–922.

Kreye VA and Reske SN (1982) Possible site of the in vivo disposition of sodium nitroprusside in the rat. *Naunyn-Schmiedeberg's Arch Pharmacol* **320:**260–265.

Kruszyna H, Kruszyna R, Rochelle LG, Smith RP, and Wilcox DE (1993) Effects of temperature, oxygen, heme ligands and sulfhydryl alkylation on the reactions of nitroprusside and nitroglycerin with hemoglobin. *Biochem Pharmacol* **46:**95–102.

Maragos CM, Morley D, Wink DA, Dunams TM, Saavedra JE, Hoffman A, Bove AA, Isaac L, Hrabie JA, and Keefer LK (1991) Complexes of NO with nucleophiles as agents for the controlled biological release of nitric oxide. Vasorelaxant effects. *J Med Chem* **34:**3242–3247.

Milani M, Ouellet Y, Ouellet H, Guertin M, Boffi A, Antonini G, Bocedi A, Mattu M, Bolognesi M, and Ascenzi P (2004) Cyanide binding to truncated hemoglobins: a crystallographic and kinetic study. *Biochemistry* **43:**5213–5221.

Murad F (1986) Cyclic guanosine monophosphate as a mediator of vasodilation. *J Clin Investig* **78:**1–5.

Nagahara N, Ito T, and Minami M (1999) Mercaptopyruvate sulfurtransferase as a defense against cyanide toxication: molecular properties and mode of detoxification. *Histol Histopathol* **14:**1277–1286.

Oral HB, George AJ, and Haskard DO (1998) A sensitive fluorometric assay for determining hydrogen peroxide-mediated sublethal and lethal endothelial cell injury. *Endothelium* **6:**143–151.

Rao DN, Elguindi S, and O'Brien PJ (1991) Reductive metabolism of nitroprusside in rat hepatocytes and human erythrocytes. *Arch Biochem Biophys* **286:**30–37.

Rochelle LG, Kruszyna H, Kruszyna R, Barchowsky A, Wilcox DE, and Smith RP (1994) Bioactivation of nitroprusside by porcine endothelial cells. *Toxicol Appl Pharmacol* **128:**123–128.

Scheffler IE (2001) Mitochondria make a come back. *Adv Drug Delivery Rev* **49:**3–26.

Smith JN and Dasgupta TP (2001) Mechanisms of nitric oxide release from nitro-vasodilators in aqueous solution: reaction of the nitroprusside ion ($[Fe(CN)5NO]^{2-}$) with L-ascorbic acid. *J Inorg Biochem* **87:**165–173.

Stamler JS (2003) Hemoglobin and nitric oxide. *N Engl J Med* **349:**402–405.

Stamler JS, Jia L, Eu JP, McMahon TJ, Demchenko IT, Bonaventura J, Gernert K, and Piantadosi CA (1997) Blood flow regulation by S-nitrosohemoglobin in the physiological oxygen gradient. *Science (Wash DC)* **276:**2034–2037.

Wilcox DE, Kruszyna H, Kruszyna R, and Smith RP (1990) Effect of cyanide on the reaction of nitroprusside with hemoglobin: relevance to cyanide interference with the biological activity of nitroprusside. *Chem Res Toxicol* **3:**71–76.

Williams DL (2003) A chemist's view of the nitric oxide story. *Org Biomol Chem* **1:**441–449.

Winterbourn CC (1990) Oxidative reactions of hemoglobin. *Methods Enzymol* **186:**265–272.

Yonetani T, Tsuneshige A, Zhou Y, and Chen X (1998) Electron paramagnetic resonance and oxygen binding studies of α-nitrosyl hemoglobin. A novel oxygen carrier having no-assisted allosteric functions. *J Biol Chem* **273:**20323–20333.

Address correspondence to: Dr. Giancarlo Aldini, Address: Istituto di Chimica Farmaceutica e Tossicologica "Pietro Pratesi", Viale Abruzzi 42, 20131 Milan, Italy. E-mail: giancarlo.aldini@unimi.it